1

Screen-Printed Electrode based Electrochemical Detector Coupled with in situ Ionic Liquid Assisted Dispersive Liquid-Liquid Microextraction for determination of 2,4,6-trinitrotoluene

Elena Fernández[1], Lorena Vidal[1*], Jesús Iniesta[2], Jonathan P. Metters[3], Craig E. Banks[3] and Antonio Canals[1*]

[1]Departamento de Química Analítica, Nutrición y Bromatología e Instituto Universitario de Materiales, Universidad de Alicante, P.O. Box 99, E-03080 Alicante, Spain.

[2]Departamento de Química Física e Instituto Universitario de Electroquímica , Universidad de Alicante, P.O. Box 99, E-03080, Alicante, Spain.

[3] Faculty of Science and Engineering, Chemistry and Environmental Science, Manchester Metropolitan University, Chester Street, Manchester M1 5GD, Lancs, United Kingdom.

*Corresponding authors: Tel.: +345909790; fax: +34965909790.

E-mail addresses: lorena.vidal@ua.es (L. Vidal), a.canals@ua.es (A. Canals).

ABSTRACT

A novel methodology is reported, whereby screen-printed electrodes (SPELs) are combined with dispersive liquid-liquid microextraction. *In situ* ionic liquid (IL) formation has been employed as an extractant phase in the microextraction technique, proving to be a simple, fast and inexpensive analytical method. This approach uses miniaturized systems both in sample preparation and detection stage, helping to develop environmentally friendly analytical methods and portable devices to allow rapid and onsite measurements. The microextraction methodology is based on a simple metathesis reaction in which a water-immiscible IL (1-hexyl-3-methylimidazolium bis[(trifluoromethyl)sulfonyl]imide, $[Hmim][NTf_2]$) is formed

from a water-miscible IL (1-hexyl-3-methylimidazolium chloride, [Hmim][Cl]) and an ion-exchange reagent (lithium bis[(trifluoromethyl)sulfonyl]imide, LiNTf$_2$) into sample solutions. The explosive 2,4,6-trinitrotoluene (TNT) has been used as model analyte to develop the method. The electrochemical behaviour of TNT in [Hmim][NTf$_2$] has been studied in SPELs. The extraction methodology was initially optimized with a two-step multivariate optimization strategy, using Plackett-Burman and central composite designs. Under the optimum conditions the method was evaluated and a good level of linearity was obtained with a correlation coefficient of 0.9990. Limits of detection and quantification were found to be 7 µg L^{-1} and 9 µg L^{-1}, respectively. The repeatability of the proposed method was evaluated at two different spiking levels (20 and 50 µg L^{-1}) and coefficients of variation of 7% and 5% (n=5) were obtained. Tap water and industrial wastewater were selected as real-world water samples in order to assess the applicability of the method.

INTRODUCTION

Miniaturization of both analytical methodologies and instrumentation has become very popular in recent years, and many efforts have focused on carrying out chemical analysis at a reduced scale. Miniaturization of sample preparation methodologies has significantly increased with the development of a great number of solid-phase and liquid-phase microextraction techniques

[1,2]. Liquid-phase microextraction (LPME) offers simplicity, ease of handling, minimal sample and solvent consumptions, and an important reduction in residues generated, in contrast with traditional liquid-liquid extraction techniques. Since its appearance in the nineties, several LPME techniques have been developed being single drop microextraction, hollow-fiber liquid-phase microextraction and dispersive liquid-liquid microextraction [3] (DLLME) the most commonly used. Although organic solvents have traditionally been used as extractants in LPME techniques, the use of ionic liquids (ILs) has recently attracted interest as a promising alternative [4]. ILs are melted salts at room temperature that possess unique properties among which we can highlight their being highly thermal and chemically stabile, with negligible vapor pressure, tunable viscosity, electrolytic conductivity, a wide electrochemical window and good extractability of organic compounds and metal ions [5]. The utilization of ILs has helped to overcome problems associated with LPME techniques using organic solvents [4] and enabled the development of new methodologies such as temperature-controlled IL dispersive liquid-liquid microextraction [6] and *in situ* IL formation dispersive liquid-liquid microextraction (*in situ* IL-DLLME) [7,8]. During *in situ* IL-DLLME the extractant phase is formed into sample solution via a metathesis reaction between a water-miscible IL and an ion exchange reagent to form a water-immiscible IL. Homogeneously dispersed fine drops of the extractant phase are generated and high enrichment factors are obtained with low extraction times due to the high contact surface between phases. Dispersion of the IL takes place via metathesis reaction, and a disperser agent is not needed, thus avoiding competition with the IL and decreasing extraction efficiency. Moreover,

77 additional devices are avoided such as vortex or ultrasound bath, which have

78 also been used to assist IL-DLLME [9,10].

79 In most cases, LPME procedures are followed by chromatographic

80 separations, in either liquid or gas modalities, coupled with different detection

81 systems (UV-Vis, inductively coupled plasma optical emission spectrometry or

82 mass spectrometry, among others). Most of these detection systems are slow,

83 expensive and bulky, so analytical instrumentation employed for detection has

84 not achieved the same degree of miniaturization as miniaturized sample

85 preparation methodologies, which are more widely used. Furthermore, ILs

86 present some disadvantages when chromatographic techniques are used. For

87 example, special devices are needed when ILs are injected in gas

88 chromatography due to their high boiling points [11,12], or shorter column life

89 and resolution problems appear in liquid chromatography. Accordingly,

90 electrochemical sensors are presented as an attractive option for use in

91 detection methodologies. Recent advances in microfabrication and screen-

92 printing technologies enable the development of miniaturized and easy-to-use

93 electrochemical systems for rapid and de-centralized onsite measurements.

94 Screen-printed electrodes [13] (SPELs) are inexpensive, mass-produced,

95 disposable devices, which are ideal for low volume sample analysis. Moreover,

96 the versatility and ease of modifying these electrodes make them advantageous

97 when improving their performance and adapting them to specific analytes.

98 To our knowledge, this is the first report of an analytical method in which

99 SPELs are used as electrochemical detector for LPME. ILs possess intrinsic

100 conductivity, a wide electrochemical window and thermal stability, therefore they

101 have been recognised as ideal alternative electrolytes in electrochemical

102 devices [14]. Taking into account the electrochemical properties of ILs and the

103 low volume of the IL-phase formed during *in situ* IL-DLLME (10-20 µL), SPELs

104 seem to be ideal and perfectly compatible candidates for analyzing IL drop after

105 microextraction without any further modification. The explosive 2,4,6-

106 trinitrotoluene (TNT) has been used as a model analyte to develop the

107 proposed methodology since its electrochemical behaviour has been widely

108 characterized. Additionally, nitroaromatic explosives, such as TNT, have

109 received increasing interest in recent years. Concerns about terrorist activity

110 have led to intensification of security measures in airports and public buildings,

111 demanding highly sensitive analytical methods to detect these compounds at

112 trace levels. Furthermore, their presence in surrounding soils, waterways and

113 reservoirs must be monitored in areas where they are produced, stored or

114 detonated. The mutagenic and toxic properties of nitroaromatic explosives

115 make their presence in the environment dangerous [15]. A great number of

116 analytical methods using gas [16], liquid [17] and micellar electrokinetic [18]

117 chromatography and immunoassay techniques [19] have been developed to

118 determine TNT and other related explosives in environmental samples.

119 However, the inherent redox activity of TNT makes electrochemical sensors a

120 very suitable alternative. Electrochemistry offers simplicity, a rapid response,

121 low-cost instrumentation with portable options, as well as analytical

122 requirements of sensitivity and reproducibility.

123   Screen-printed electrodes have previously been used in electrochemical

124 devices for TNT analysis. Hydrogel-coated SPELs have been used to detect

125 thermally desorbed TNT from an integrated preconcentration system for both

126 solid and liquid samples [20]. An electrochemically pre-anodized Nafion-coated

127 screen-printed carbon electrode (SPCE) has been used in a disposable sensor

128 developed to determine different nitroaromatic compounds [21]. With this

129 system, TNT can be detected in spiked lake water at a concentration of 30 μM

130 (6.8 μg mL^{-1}). A wearable textile-based screen-printed electrochemical sensor,

131 which is highly suitable for monitoring the surroundings of the wearer, has been

132 tested to detect nitroaromatic explosives both in gas and liquid phase, obtaining

133 a limit of detection (LOD) of around 1 μg mL^{-1} for TNT in water [22]. Recently, a

134 very simple and low-cost sensor based on unmodified SPCEs has been

135 described to determine TNT and 2,4-dinitrotoluene in aqueous solutions,

136 obtaining LODs as low as 0.4 μM (90 μg L^{-1}) and 0.7 μM (73 μg L^{-1}),

137 respectively [23].

138   The research presented here combines the advantages of LPME

139 techniques with the benefits that SPELs offer as electrochemical sensors. The

140 resulting novel methodology includes miniaturized systems in both sample

141 preparation and in detection stage. In addition, the use of an IL as extractant

142 phase not only provides the advantage of good extractability of organic

143 compounds, but also provides the electrolyte behaviour needed for detection.

144 The proposed method has been optimized using a multivariate optimization

145 strategy and has been evaluated in order to demonstrate its applicability to

146 determine TNT in real-world water samples.

147

148 **EXPERIMENTAL SECTION**

149   **Reagents and real-world water samples.** A TNT standard of 1000 mg

150 L^{-1} in acetonitrile was obtained from LGC Standards (Warsaw, Poland). Stock

151 solution of TNT (10 mg L^{-1}) was prepared in acetonitrile HPLC grade from

Sigma-Aldrich (Seelze, Germany) and stored in the dark at 4°C. Working

solutions were prepared daily by proper dilution of this stock solution in

ultrapure water from a water purification system (Mili-Q Biocel A10) supplied by

Milipore (Bilerica, MA, USA). ILs 1-hexyl-3-methylimidazolium

bis[(trifluoromethyl)sulfonyl]imide ([Hmim][NTf$_2$]) (98%) and 1-hexyl-3-

methylimidazolium chloride ([Hmim][Cl]) (98%) were purchased from Iolitec

(Heilbronn, Germany). The lithium bis[(trifluoromethyl)sulfonyl]imide (LiNTf$_2$)

salt was supplied by Sigma-Aldrich (St. Louis, MO, USA) and NaCl reactive

grade was from ACS Scharlau (Barcelona, Spain).

Tap water from a drinking water treatment plant in Seville (Spain) and

industrial wastewater from Ourense (Spain) were utilized as real-world water

samples. The industrial wastewater contained a chemical oxygen demand of

1004 mg O$_2$ L^{-1}, a biochemical oxygen demand of 278 mg O$_2$ L^{-1} and 429 mg L^{-1}

of suspended solids. Samples were collected in amber glass containers and

stored in the dark at 4°C. Tap water was used without any further pretreatment

whereas the wastewater was filtered with a 0.22 μm pore-size nylon filter before

use. The real-world water samples were previously analyzed and the target

analyte was not detected.

***In situ* IL-DLLME procedure.** Under optimum conditions, 32 mg of

[Hmim][Cl] were placed in a conical-bottom glass tube and dissolved in 11 mL

of aqueous standards or sample solutions. An equimolar quantity of LiNTf$_2$

(45.3 mg) relative to [Hmim][Cl] was added and a cloudy solution was

immediately formed. The mixture was manually shaken for 0.5 minutes. In order

to accelerate phases separation, the tube was then introduced in an ice bath for

3 minutes. Next, the phases were separated by centrifugation for 5 minutes at

177 4000 rpm. The aqueous phase was removed with a glass pipette, and 15 μL of

178 the formed IL-phase (*i.e.,* [Hmim][NTf$_2$]) was withdrawn with a syringe. Finally,

179 this 15 μL was deposited on the screen-printed graphite electrode (SPGE)

180 surface for electrochemical detection. The procedure is described in Figure 1.

181 **Electrochemical analysis.** A μ-Autolab III potentiostat/galvanostat from

182 Eco Chemie (Utrecht, The Netherlands) controlled by Autolab GPEs software

183 version 4.9 for Windows XP was used for electrochemical experiments. All

184 measurements were carried out using three electrode configuration SPGEs

185 from Kanichi Research Services Ltd. (Manchester, UK). SPGEs were

186 manufactured as previously described [24]. The working electrode, 3.1 mm

187 diameter, and the counter electrode were made of a graphite ink. A pseudo

188 Ag/AgCl was the reference electrode. Connectors for the electrochemical

189 connection of the SPGEs were also obtained from Kanichi Research Services

190 Ltd. SPGEs were used without any pretreatment or modification of the working

191 electrode surface and a new SPGE was used for each experiment.

192 Differential pulse voltammetry (DPV) was selected as the electroanalytical

193 technique. Various DPV parameters were optimized with a once-at-a-time

194 strategy, selecting the following optimum conditions: 100 mV modulation

195 amplitude; 10 mV step potential; 0.05 s modulation time and 0.5 s interval time.

196 Pure N$_2$ from Air Liquide (Madrid, Spain) was flowed for 20 minutes before DPV

197 experiments and maintained during measurements. The signal corresponding to

198 oxygen embedded in the IL [25] appears at the same reduction potential as the

199 analyte, therefore, purging with N$_2$ was necessary to ensure a deoxygenated

200 atmosphere in which the analyte could be detected at low concentrations. All

201 electrochemical measurements were carried out at room temperature.

202 **Data processing.** The current peak of the first cathodic wave of TNT at -

203 0.80 V *vs* pseudo Ag/AgCl was used to identify and quantify the analyte in order

204 to evaluate the developed method. A multivariate optimization strategy was

205 carried out to determine the optimum conditions of the microextraction

206 methodology. Statgraphics Statistical Computer Package "Statgraphics Plus

207 5.1." (Warrenton, VA, USA) was used to construct the experimental design

208 matrices and evaluate the results.

209

210 **RESULTS AND DISCUSSION**

211 **Multivariate optimization**

212 **Screening step.** Plackett-Burman design is a two-level fractional

213 factorial design for studying k=N-1 variables in N runs, where N is a multiple of

214 4 [26]. Fractional factorial designs are very useful in the first steps of a project

215 when many variables are initially considered but only a few show important

216 effects. The Plackett-Burman design ignores interaction between variables so

217 the main effects can be calculated with a reduced number of experiments,

218 thereby leading to more economical experimentation. A saturated Plackett-

219 Burman design was used to construct the matrix of experiments, including 11

220 variables: eight real variables and three dummy variables. The effects of

221 dummy variables were used to evaluate the experimental error [27,28].

222 Based on the literature and previous experience of the research group

223 [7,29], the eight real experimental variables selected at two levels were: amount

224 of [Hmim][Cl], sample volume, molar ratio between [Hmim][Cl] and the salt

225 LiNTf$_2$, ionic strength, extraction time, centrifugation speed, centrifugation time

226 and purge time with N$_2$ before electrochemical measurements. Table 1 shows

227   the experimental variables and levels considered in the Plackett-Burman

228   design. A total of twelve experiments were carried out using aqueous standards

229   of 100 µg L^{-1}.

230   The data obtained were evaluated using an ANOVA test and the results

231   were visualized with the Pareto chart shown in Figure S1(a) (see Electronic

232   Supplementary Material). The length of each bar was proportional to the

233   influence of the corresponding variable and the effects that exceed the

234   reference vertical line can be considered significant with a 95% probability.

235   According to Figure S1(a), only the amount of [Hmim][Cl] was a

236   statistically significant variable, with 95% probability, having a negative effect.

237   This negative effect is in agreement with the fact that if a lower amount of

238   [Hmim][Cl] is used, a smaller volume of IL-phase is formed in the

239   microextraction procedure, thus a higher concentration of the analyte is

240   obtained in the extraction phase.

241   Sample volume is the second most important variable having a non-

242   significant positive effect but being much larger than purge time. According to

243   our previous experience, sample volume is an important variable to consider in

244   microextraction techniques. In general, greater sample volume involves a

245   greater amount of analyte and therefore increases the response. For this

246   reason, both the amount of [Hmim][Cl] and sample volume were selected as the

247   main variables affecting the response of the system, and were investigated in

248   the optimization of the significant variables step. The other six real variables

249   with non-significant effects were fixed at the most experimentally convenient

250   level (namely stoichiometric molar ratio between [Hmim][Cl] and LiNTf$_2$; ionic

251 strength: 0% NaCl; extraction time: 0.5 min; centrifugation speed: 4000 rpm;

252 centrifugation time: 5 min; and purge time: 20 min).

253 **Optimization of significant variables.** Central composite design (CCD)

254 was employed in this optimization step. This design combines a two-level full

255 factorial design (2^k) with 2k star points, where k is the number of variables being

256 optimized, and one point at the center of the experimental region, that can be

257 run n times. In order to ensure the rotatability of the model, star points were set

258 at $\alpha=\sqrt{k}=1.41$ whereas the central point was repeated five times to provide an

259 orthogonal design [26]. CCD was used to evaluate and optimize main effects,

260 interaction effects and quadratic effects of the two considered variables. Table 2

261 shows the low and high levels, the central and star points of the considered

262 variables in the optimization step. Thirteen experiments were carried out using

263 aqueous standards of 100 µg L^{-1}.

264 The data obtained were also evaluated using an ANOVA test and the

265 results were visualized with the Pareto chart shown in Figure S1(b) (Electronic

266 Supplementary Material). As can be seen, both the amount of [Hmim][Cl] and

267 sample volume were significant variables, with a 95% probability, confirming the

268 predicted importance of sample volume effect. One of the quadratic effects was

269 also significant, assuming the curvature of the system and fitting the second-

270 grade polynomial model proposed. The response surface obtained using the

271 CCD is shown in Figure 2. The surface graph shows a pronounced increase in

272 the analytical signal as the amount of [Hmim][Cl] decreases and sample volume

273 increases.

274 In summary, the results obtained from the optimization process lead to

275 the following experimental conditions: amount of [Hmim][Cl], 32 mg; sample

276   volume, 11 mL; molar ratio [Hmim][Cl]:LiNTf$_2$, 1:1; ionic strength, 0% NaCl;

277   extraction time, 0.5 min; centrifugation speed, 4000 rpm; centrifugation time, 5

278   min; and purge time before electrochemical measurements, 20 min.

279   **Electrochemical study of TNT in [Hmim][NTf$_2$] at SPGEs.** DPV of a

280   blank and four TNT standards of 10, 30, 50 and 70 mg L^{-1} prepared in

281   commercial [Hmim][NTf$_2$] were carried out using SPGEs in order to study the

282   electrochemical behavior of the analyte. According to previous studies [30,31] ,

283   using ILs as electrolytes generally leads to three consecutive reduction peaks of

284   TNT, which are believed to correspond to each nitro group at the aromatic ring.

285   Figure 3 shows DPV curves obtained in this study. As can be observed, a well-

286   defined cathodic peak appears at -0.80 V, corresponding to the reduction of one

287   of the three nitro groups in the molecule, whereas the two peaks corresponding

288   to the remaining nitro groups cannot be clearly distinguished. The current peak

289   at -0.80 V displayed a good linearity, between 10 and 70 mg L^{-1}, with a

290   correlation coefficient (r) of 0.996. The repeatability of the electrochemical

291   response was also evaluated for five repeated analyses of the 70 mg L^{-1}

292   standard and a coefficient of variation (CV) value of 2% was found.

293   Secondly, the electrochemical behavior of TNT in [Hmim][NTf$_2$] generated *in

294   situ* was studied. As shown in Figure 4, the reduction peaks of the three nitro

295   groups are perfectly well-defined and, as in commercial [Hmim][NTf$_2$], an

296   identical peak appears at -0.80 V. Nevertheless, the reductive peaks at -1.06 V

297   and -1.27 V are not well-defined at lower concentrations, therefore the current

298   peak at -0.80 V was finally chosen for evaluation of the proposed method.

299   **Analytical figures of merit of the proposed method.** Quality

300   parameters of the proposed method were evaluated. A concentration range

301   from 10 to 100 µg L^{-1} was studied and the linear range was finally established

302   from 10 to 80 µg L^{-1}. The resulting calibration curve gave a high level of linearity

303   with a correlation coefficient (r) of 0.9990 (N=4). The sensitivity of the

304   instrumental measurements estimated by the slope of the calibration curve was

305   (0.0112 ± 0.0004) µA µg^{-1} L. The repeatability of the proposed method,

306   expressed as CV, was evaluated at two different spiking levels (20 and 50 µg L^{-}

307   ^{1}) by extracting five consecutive aqueous standards, and CV values were found

308   to be 7% and 5%, respectively. The enrichment factor of the proposed

309   procedure was 300, defined as the ratio of C_o/C_a, where C_o is the concentration

310   of analytes in the IL phase after extraction and C_a is the original concentration

311   of analytes in the aqueous phase.

312   The LOD and the limit of quantification (LOQ) were estimated using the

313   mean signal of the blank (n=three replicates) at -0.80 V plus three or ten times

314   its standard deviation. The LOD was found to be 7 µg L^{-1} whereas the LOQ was

315   9 µg L^{-1}. It should be pointed out that the LOD of the developed method is equal

316   or even lower than others recently reported detection limits for the

317   electrochemical analysis of TNT obtained with more expensive and complex

318   electrodes, using carbon nanomaterials, metallic nanoparticles or assembly

319   procedures (Table 3). In addition, our approach combines a simple sample

320   preparation step with unmodified inexpensive SPGEs, thereby providing a lower

321   LOD than those obtained with other SPELs [20-23] reported to date (Table 3);

322   therefore the developed method presents unique benefits.

323   **Real-world water samples analysis.** The applicability of the proposed

324   method to determine TNT in real-world water samples was evaluated. Three

325   replicated analyses of both tap water and wastewater were carried out at 40 µg

326 L^{-1} spiking level. Wastewater was filtered with a 0.22 μm nylon filter after being

327 spiked. It should be noted that in previous analyses none of the selected water

328 samples had initial detectable TNT concentrations. Relative recoveries were

329 calculated as the ratio of the signals found in real and ultrapure water samples

330 spiked at the same concentration level. Relative recovery for tap water samples

331 was found to be 114% with a CV value of 16%, whereas for wastewater

332 samples the relative recovery was 109% with 18% CV. According to these

333 results, it can be concluded that the matrix effects were not significant in TNT

334 analysis in the two selected water samples. Therefore, the developed method

335 can be successfully applied to clean and complex water sample matrices.

336

337 **CONCLUSIONS**

338 Screen-printed graphite electrode-based electrochemical detection has

339 been successfully combined with LPME for the first time. The proposed

340 analytical method employs miniaturized systems both in sample preparation

341 and in detection stage, with the advantage of avoiding expensive and bulky or

342 immovable instrumentation. *In situ* IL formation in the microextraction

343 methodology avoids the use of harmful and toxic organic compounds both as

344 extractant and disperser solvents. The incorporation of a simple and fast

345 sample preparation step before the electrochemical measurements with low-

346 cost and disposable SPGEs has yielded a lower LOD than the detection limits

347 previously reported for other SPELs. The multivariate optimization strategy used

348 here enabled us to rapidly and economically find the optimum conditions for the

349 main experimental parameters involved in the sample preparation method, thus

350 providing complete information. Finally, the results have proven the applicability

351 of the proposed method to determine TNT at trace levels in real-world water
352 samples. Although the use of a nitrogen purge, ice bath and the centrifuge
353 presents a limitation to the portability, this methodology provides a step forward
354 in the development of portable and economical systems available to any
355 laboratory.

356

357 **ACKNOWLEDGMENTS**

362

REFERENCES

364 1. Risticevic S, Niri VH, Vuckovic D, Pawliszyn J (2009) Anal Bioanal Chem 393:781–
365 795.

366 2. Pena-Pereira F, Lavilla I, Bendicho C (2010) Trends Anal Chem 29:617–628.

367 3. Rezaee M, Assadi Y, Milani Hosseini M-R, Aghaee E, Ahmadi F, Berijani S (2006) J
368 Chromatogr A 1116:1–9.

369 4. Aguilera-Herrador E, Lucena R, Cárdenas S, Valcárcel M (2010) Trends Anal Chem
370 29:602–616.

371 5. Sun P, Armstrong DW (2010) Anal Chim Acta 661:1–16.

372 6. Zhou Q, Bai H, Xie G, Xiao J (2008) J Chromatogr A 1177:43–49.

373 7. Baghdadi M, Shemirani F (2009) Anal Chim Acta 634:186–191.

374 8. Yao C, Anderson JL (2009) Anal Bioanal Chem 395:1491–1502.

375 9. Sun X-M, Sun Y, Wu L-W, Jiang C-Z, Yu X, Gao Y, Wang L-Y, Song D-Q (2012)
376 Anal Methods 4:2074–2080.

377 10. Zhang Y, Lee HK (2012) Anal Chim Acta 750:120–126.

378 11. Aguilera-Herrador E, Lucena R, Cárdenas S, Valcárcel M (2008) Anal Chem
379 80:793-800

380 12. Chisvert A, Román IP, Vidal L, Canals A (2009) J Chromatogr A 1216:1290-1295.

381 13. Metters JP, Kadara RO, Banks CE (2011) The Analyst 136:1067–1076.

382 14. Buzzeo MC, Evans RG, Compton RG (2004) Chemphyschem 5:1106–1120.

383 15. Pichtel J (2012) Appl Environ Soil Sci 2012:1–33.

384 16. Cortada C, Vidal L, Canals A (2011) Talanta 85:2546–2552.

385 17. Sun Q, Chen Z, Yuan D, Yuan D, Yu C-P, Mallavarapu M, Naidu R (2011)
386 Chromatographia 73:631–637.

387 18. Giordano BC, Burgi DS, Collins GE (2010) J Chromatogr A 1217:4487–4493.

388 19. Goldman ER, Anderson GP, Lebedev N, Lingerfelt BM, Winter PT, Patterson CH,
389 Mauro JM (2003) Anal Bioanal Chem 375:471–475.

390 20. Cizek K, Prior C, Thammakhet C, Galik M, Linker K, Tsui R, Cagan A, Wake J, La
391 Belle J, Wang J (2010) Anal Chim Acta 661:117–121.

392

393 21. Chen J-C, Shih J-L, Liu C-H, Liu C-H, Kuo M-Y, Zen, J-M (2006) Anal Chem
394 78:3752–3757.

395 22. Chuang M-C, Windmiller JR, Santhosh P, Santhosh P, Ramirez GV, Galik M, Chou
396 T-Y, Wang J (2010) Electroanalysis 22:2511–2518.

397 23. Caygill JS, Collyer SD, Holmes JL, Davis F, Higson S (2013) The Analyst 138:346–
398 352.

399 24. Hallam PM, Kampouris DK, Kadara RO, Banks CE (2010) The Analyst 135:1947–
400 1952.

401 25. Lee J, Murugappan K, Arrigan DWM, Silvester DS (2012) Electrochim Acta
402 101:158-168.

403 26. Montgomery DC (2009) Design and Analysis of Experiments, 7th ed. Wiley, New
404 Jersey.

405 27. Heyden YV, Hartmann C, Massart DL, Michel L, Kiechle P, Erni F (1995) Anal
406 Chim Acta 316:15–26.

407 28. Fabre H, Mesplet N (2000) J Chromatogr A 897:329–338.

408 29. Cortada C, Vidal L, Canals A (2011) J Chromatogr A 1218:17–22.

409 30. Rabenecker P, Pinkwart K (2009) Propellants Explos Pyrotech 34:274–279.

410 31. Xiao C, Rehman A, Zeng X (2012) Anal Chem 84:1416–1424.

411 32. Zhang H-X, Cao A-M, Hu J-S, Wan L-J, Lee S-T (2006) Anal Chem78:1967–1971.
412
413 33. Zang J, Guo CX, Hu F, Yu L, Li CM (2011) Anal Chim Acta 683:187–191.

414 34. Wang J, Hocevar SB, Ogorevc B (2004) Electrochem Commun 6:176–179.

415 35. Hrapovic S, Majid E, Liu Y, Male K, Luong J (2006) Anal Chem 78:5504–5512.

416 36. Shi G, Qu Y, Zhai Y, Liu Y, Sun Z, Yang J, Jin L (2007) Electrochem Commun
417 9:1719–1724.

418 37. Wang J, Pumera M (2006) Talanta 69:984–987.

419 38. Agüí L, Vega-Montenegro D, Yáñez-Sedeño P, Pingarrón JM (2005) Anal Bioanal
420 Chem 382:381–387.

421 39. De Sanoit J, Vanhove E, Mailley P, Bergonzo P (2009) Electrochim Acta 54:5688–
422 5693.

423 40. Tan SM, Chua CK, Pumera M (2013) The Analyst 138:1700–1704.

424

425

Figure Captions

Fig. 1 *in situ* IL-DLLME coupled with SPGE

Fig. 2 Response surface of CCD

Fig. 3 DPV curves of a blank and four TNT standards prepared in commercial [Hmim][NTf$_2$]

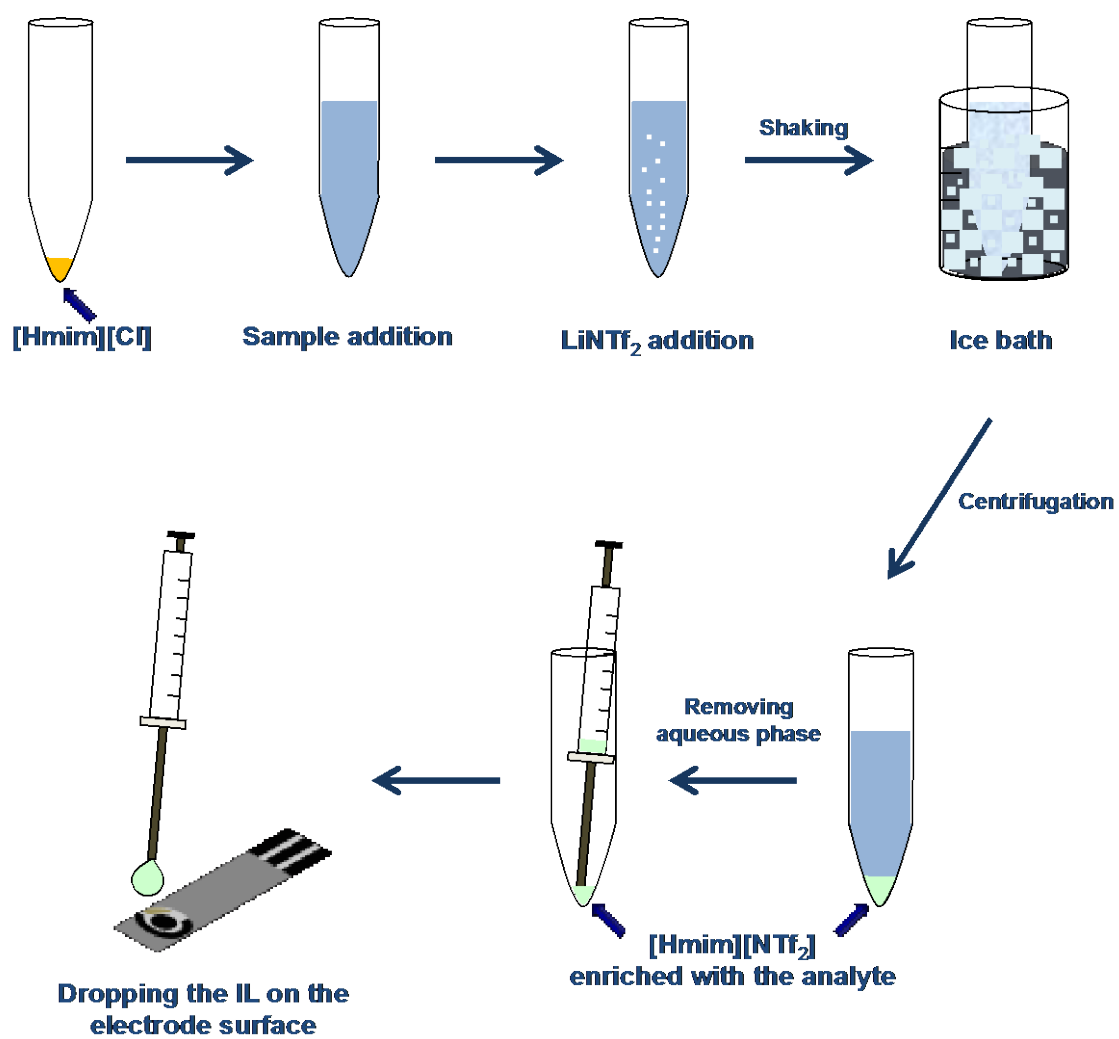**Fig. 4** DPV curves of a blank and a TNT standard of 80 µg L^{-1} in ultrapure water after *in situ* IL-DLLME under optimum conditions
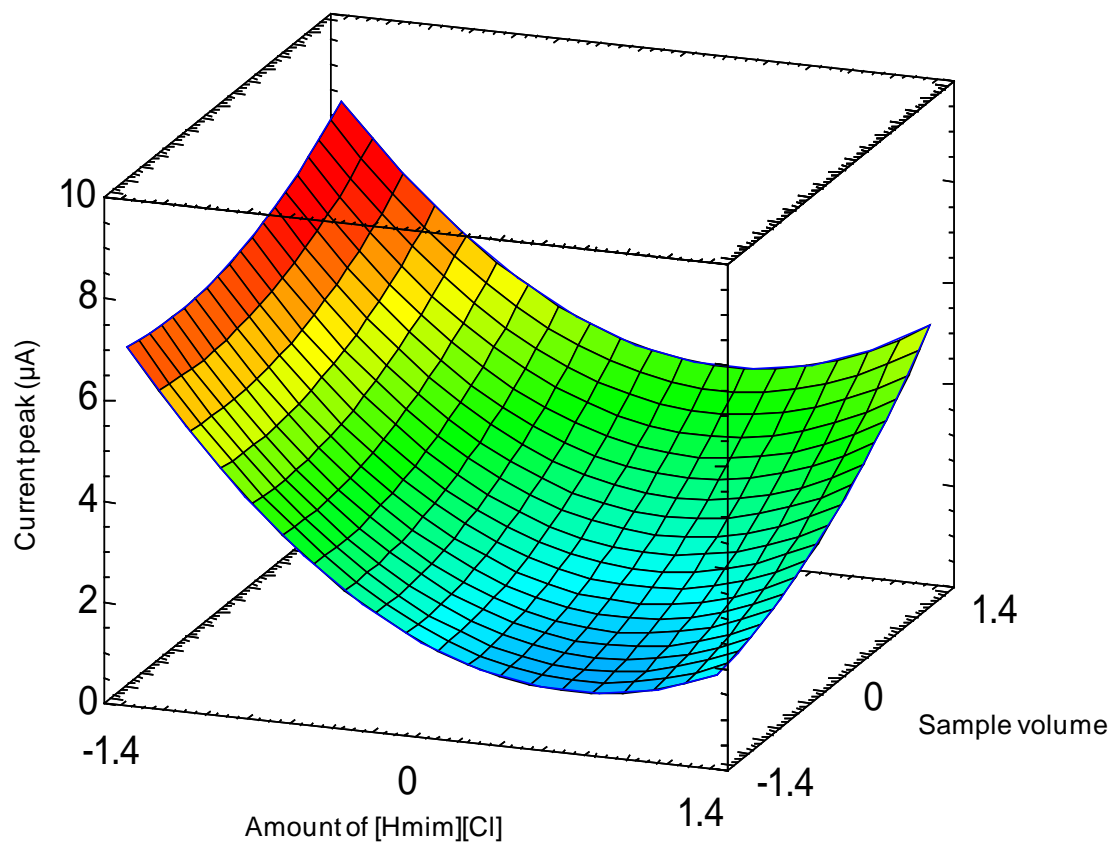
435

Fig. 1

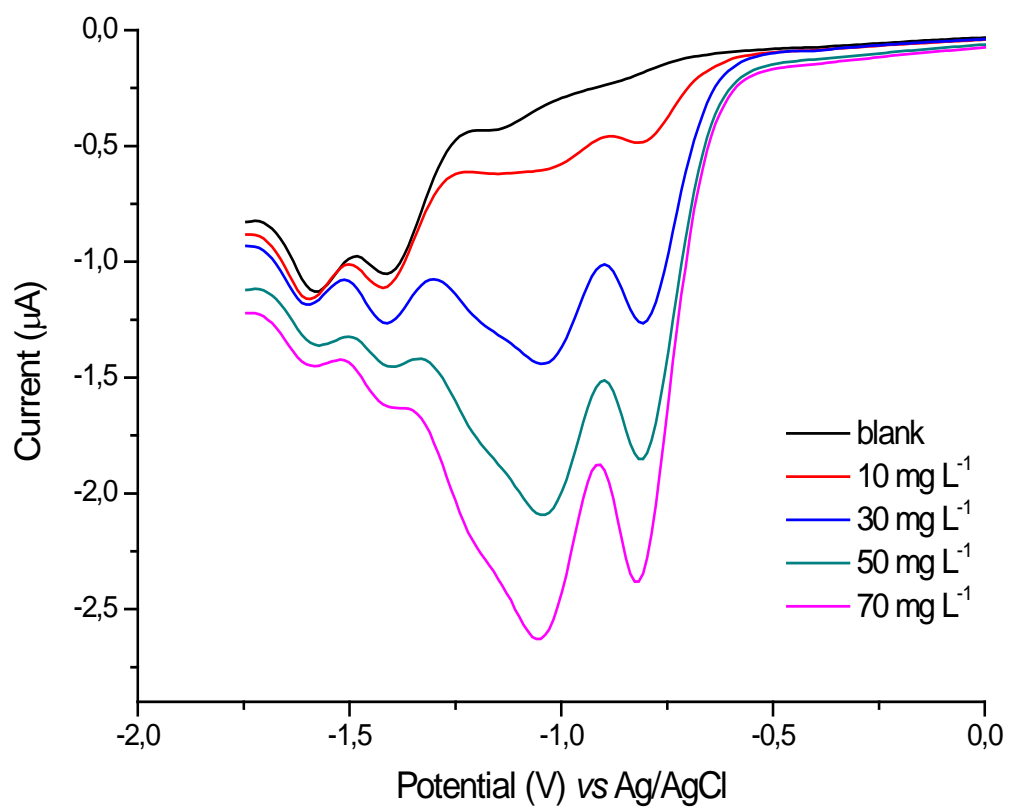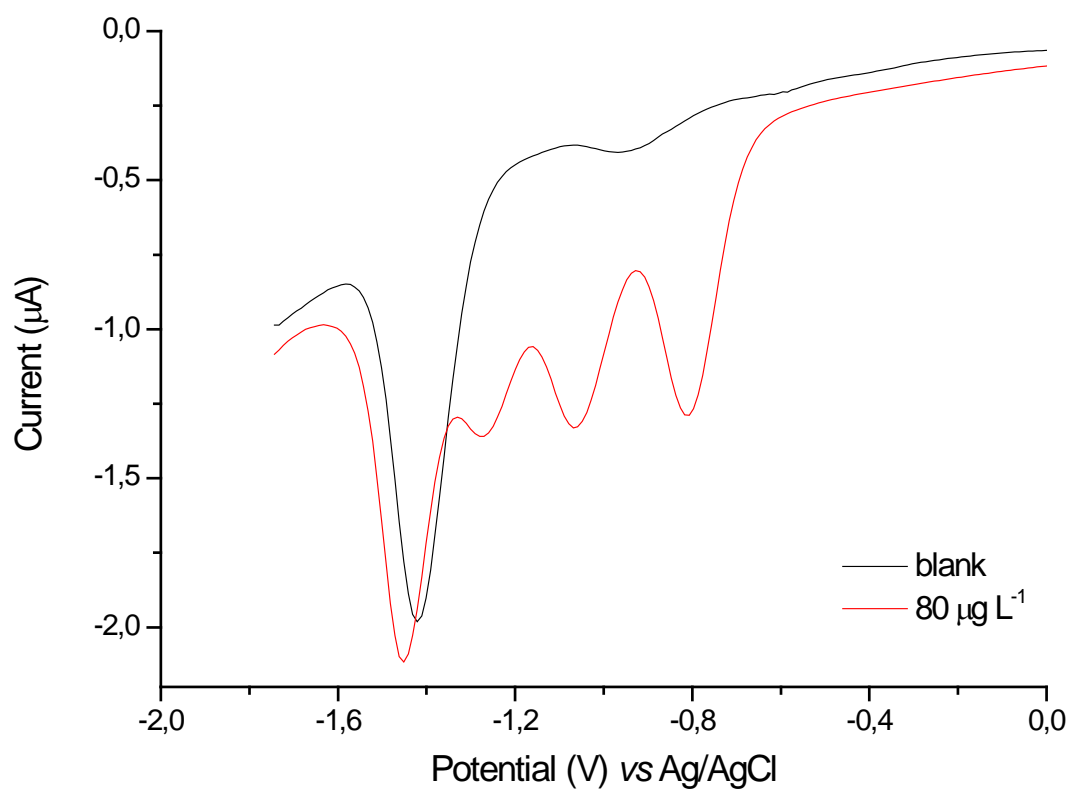[Hmim][Cl] → Sample addition → LiNTf$_2$ addition → Shaking → Ice bath

Centrifugation

Dropping the IL on the electrode surface ← Removing aqueous phase ← [Hmim][NTf$_2$] enriched with the analyte

436

437

438

Fig. 2

439

440

Fig. 3

Fig. 4

445 **Table 1.** Experimental variables and levels of the Plackett-Burman design.

Variable	Level	
	Low (-1)	High (+1)
Amount of [Hmim][Cl] (mg)	34	68
Sample volume (mL)	5	11
Ionic strength (NaCl concentration, %, w/v)	0	10
Molar ratio [Hmim][Cl]:LiNTf$_2$	1:1	1:3
Extraction time (min)	0.5	1
Centrifugation time (min)	5	10
Centrifugation speed (rpm)	2000	4000
Purge time (min)	20	30

446

447 **Table 2.** Variables, low and high levels, central and star points used in CCD.

Variable	Level			Star points (α=1.41)	
	Low (-1)	Central (0)	High (+1)	-α	+α
Amount of [Hmim][Cl] (mg)	40	60	80	32	88
Sample volume (mL)	4	7	10	3	11

448 **Table 3.** Characteristics of some electrochemical methods developed to determine TNT and

449 other nitroaromatic explosives.

Electrode	Analytical technique	Analytes	Real samples and spiking levels in parenthesis	TNT LOD	Ref
SPGE	DPV	TNT	Tap water and industrial wastewater (40 µg L^{-1})	7 µg L^{-1}	This work
Hydrogel-coated SPEL	SWV	TNT	-	-	[20]
Nafion-coated SPCE	SWV	TNT and other nitroaromatic explosives	Lake water (30 µM; 6.8 µg mL^{-1})	-	[21]
Textile-based SPEL	SWV	TNT and 2,4-dinitrotoluene	-	1 µg mL^{-1}	[22]
SPCE	CV	TNT and 2,4-dinitrotoluene	-	0.4 µM (90 µg L^{-1})	[23]
Mesoporous SiO$_2$ modified GCE	LSV	TNT and other nitroaromatic explosives	-	< 1.8 nM (4 µg L^{-1})	[32]
GCE functionalized with OMC	AdsSV	TNT and other nitroaromatic explosives	-	0.2 µg L^{-1}	[33]
GCE modified with MWCNTs	AdsSV	TNT	Sea water (100-1000 µg L^{-1})	0.6 µg L^{-1}	[34]
GCE modified with Cu nanoparticles and SWCNTs	AdsSV	TNT and other nitroaromatic explosives	River and tap water, and soil (50-200 µg L^{-1})	1 µg L^{-1}	[35]
GCE modified by LbL self-assembled of {MSU/PDDA}n films.	DPV	TNT and other nitroaromatic explosives	-	1.5 nM (3.4 µg L^{-1})	[36]
Amalgam Hg/Au electrode	Microchip FIA- ED	TNT	-	7 µg L^{-1}	[37]
Electrochemically activated CFMEs	SWV	TNT and other nitroaromatic explosives	Tap and ground water (2 mg L^{-1}); soil samples (200 mg g^{-1})	0.03 µg mL^{-1}	[38]
BDD	SWV	TNT	Sea water (20-400 µg L^{-1})	10 µg L^{-1}	[39]
Graphene nanoribbon-modified GCE, graphene nanosheet-modified GCE and bare GCE	DPV	TNT	Sea water (4-20 mg L^{-1})	0.140-0.520 mg L^{-1}	[40]

450 DPV, diferential pulse voltammetry; GCE, glassy carbon electrode; LSV, linear sweep

451 voltammetry; OMC, ordered mesoporous carbon; AdsSV, adsorptive stripping voltammetry;

452 MWCNTs, multi-wall carbon nanotubes; SWCNTs single-wallet carbon nanotubes; LbL, layer-

453 by-layer; MSU, mesoporous SiO$_2$; PDDA, poly(diallyldimethylammonium) chloride; FIA-ED, flow

454 injection analysis with electrochemical detection; CFMEs, carbon fiber microelectrodes; SWV,

455 square wave voltammetry; CV, cyclic voltammetry; BDD, boron doped diamond.